Journal of Multidisciplinary Engineering Science and Technology (JMEST)
ISSN: 2458-9403
Vol. 10 Issue 9, September - 2023

Modeling of Heat and MassTransfer around a Rotating Cone of Revolution

BEZANDRY Germain
Laboratory of Mechanics Energetic and Environment (LMEE)
University of Fianarantsoa, Madagascar
tinirisoa77@gmail.com

FANJIRINDRATOVO Tovondahiniriko
Laboratory of Physics and dEnvironment
University of Toliara, Madagascar
fanjiry@gmail.com

Belkacem ZEGHMATI
LAboratoire de Modélisation Pluridisciplinaire et Simulations. Groupe de Mécanique Energétique
University of Perpignan Via Domitia, France
zeghmati@univ-perp.fr

Marcelin Hajamalala ANDRIANANTENAINA
Laboratory of Mechanics Energetic and Environment (LMEE)
University of Fianarantsoa, Madagascar
hajamalalaa@yahoo.fr

***Abstract*— Heat and mass transfers around a rotating cone immersed in air with respect to its axis of revolution are numerically investigated by using a model based on the heat and mass transfer's equations, on the continuity equation and the Navies-Stokes equations. An implicit finite difference scheme was used to discretize the equations of the mathematical model. The discretized equations were solved by Thomas's algorithm associated with the boundary conditions. A numerical code was developed. The profiles of the dimensionless values relating to the meridian, azimuthal and normal components of the velocity, of the temperature and of the mass concentration distributions in the boundary layer as well as the numbers of Nusselt, Sherwood and mass diffusion rate with relative humidity have been presented. In addition, the influence of angular velocity on the local Nusselt number, Sherwood number and mass diffusion is analyzed. A dimensionless correlation of the Nusselt and Sherwood number by the least squares method based on curves of Nusselt and Sherwood as a function of the meridian coordinate has been established.**

Keywords—modeling; heat transfer; mass transfer; rotating; cone of revolution

I. INTRODUCTION

The problem of heat and mass transfer around rotationally symmetric bodies has become of practical importance in the design of many types of industrial equipment. Convection around a cone of revolution has been a subject of research for several authors. Further, Himasekhar et al. [1] have studied an analytical the mixed rotational and natural convection around a vertical cone. Their study is based on the influence of Prandtl (Pr) number for $0.1 \leq Pr \leq 1000$ on the fluid flow and heat transfer. They have determined the predominance of the flow for $0.01 \leq$ Richardson number ≤ 100. Their results have shown that the normal and azimuthal components of velocity increase with Prandtl number while the tangential component and temperature decrease. The heat transfer rate is an increasing function of Richardson number. Similarly, the heat exchange is more important for a large value of Prandtl number. They have proposed correlations of the local Nusselt number for the three types of convection preponderance. On the other hand, Wang et al. [2] have also studied mixed convection from a rotating cone with variable surface temperature. They have shown that the maximum of the meridian velocity approaches the wall when the natural phenomenon is less dominant. It rises with increasing cone speed. The gradient of the dimensionless temperature at the wall increases uniformly with increasing cone speed. In an early work, Hering and Grosh [3] presented a numerically study mixed natural and rotational convection around a rotating vertical cone for Prandtl (Pr) number Pr = 0.7. They have examined the Richardson number to determine a zone where each convection is dominant. They have made it clear in their study that the predominance of convection is dependent on the value of Richardson number. Malik et al. [4] have studied a mixed convection dissipative viscous fluid flow over a rotating cone by way of variable viscosity and thermal conductivity. Increasing the Richardson number increases the meridian component of the velocity. The temperature of the fluid decreases with increasing Richardson number but increases with increasing Eckert number. The heat transfer and the friction coefficient increase with increasing Richardson number. Besides, Anilkumar and Roy [5] have made study about an unsteady mixed convection around a rotating cone immersed in a rotating fluid coupled with mass transfer. Increasing Prandtl and Schmidt numbers causes the thermal and mass boundary layer thicknesses to decrease respectively. The increase in buoyancy number promotes fluid adhesion and amplifies the heat and mass transfer rates. More recently, Saleem [6] has studied a heat and mass transfer around a rotating cone by mixed natural and forced convection. He has shown that the friction coefficients increase with increasing buoyancy ratio number. The Nusselt and

Sherwood numbers vary in the same way and increase with increasing buoyancy ratio. Recently, Sharma and Konwar [7] have studied heat and mass transfers around a rotating vertical cone with a permeable wall. They have presented the influence of thermal radiation and chemical reaction on heat and mass transfer respectively. They have shown that the tangential velocity and temperature of the fluid reduce as the value of the radiation parameter is increased while its concentration increases. Furthermore, Patil and Pop [8] fixed their mind closely upon the effects of surface mass transfer on unsteady mixed convection flow over a vertical cone with chemical reaction. The magnitudes of the velocity overshoot increase with the buoyancy assisting parameter, while it reduces as Prandtl number increases. The magnitude of the concentration profiles increases when the chemical reaction parameter is increased. The concentration boundary layer decreases as Schmidt number increases. Moreover, Ching [9] has swotted a free convection heat transfer from a non-isothermal permeable cone with suction and temperature dependent viscosity. The temperature of the fluid decreases as the dynamic viscosity decreases while the velocity increases. In addition, the heat transfer rate increases with decreasing dynamic viscosity. In addition, Srinivasa and Eswara [10] have investigated the unsteady free convection flow and heat transfer from an isothermal truncated cone with variable viscosity. Results have shown that the effect of variable fluid properties is to decrease both friction coefficient and Nusselt number as compared to the constant fluid properties. Velocity increases sharply near the wall whereas temperature decreases, with increase of viscosity variation parameter. Again, Bapuji et al. [11] have developed the unsteady laminar natural convection flow past an isothermal vertical cone. The tangential component of buoyancy force reduces as the semi vertical angle increases. The temperature increase with increasing semi vertical angle. Local skin friction and local Nusselt number decrease with increasing semi vertical angle. Kumari et al. [12] have treated the problem of combined free and forced convection flow along an isothermal vertical cone. Results have shown that friction coefficient and Nusselt number have increased when natural convection has predominated. On top of that, Bapuji and Chamkha [13] have presented numerical solutions of unsteady laminar free convection from a vertical cone with non uniform surface heat flux. The temperature value and thermal boundary layer thickness increase on increasing the values of semi vertical angle of the cone. Local skin-friction decreases with increasing the values of semi vertical angle of the cone. Local Nusselt number values decrease with increasing the values of semi vertical angle of the cone as temperature distribution increases with the values of semi vertical angle of the cone. Increasing the values of semi vertical angle of the cone to decrease the impulsive force along the cone surface. Another point is Azad et al. [14] have considered the natural convection flow along the vertical wavy cone in case of uniform surface heat flux where viscosity is an exponential function of temperature. Increases of viscosity variation parameter decrease the tangential velocity inside the boundary layer. The temperature inside the boundary layer at any fixed point enhanced with viscosity variation parameter. The skin friction increases vary rapidly when viscosity variation parameter increases. In a recent study, Sharaban et al. [15] have studied a natural convection along a vertical cone with uniform surface heat flux for temperature dependent thermal conductivity. Results have shown that the increasing the value of thermal conductivity variation parameter affect isotherm and leads to thicker thermal boundary layer. Bapuji et al. [16] have analyzed the unsteady laminar free convection from a vertical cone with uniform surface heat flux. The tangential component of buoyancy force reduces as the semi vertical angle increases. The temperature and boundary layer thickness increase with increasing the values of semi vertical angle of the cone. Local Nusselt number values decrease with increasing semi vertical angle. Apart from that, Lin [17] has studied the laminar free convection from a vertical cone with uniform surface heat flux. He has determined the dimensionless wall temperature distribution and wall skin friction distribution for 0.5≤ Prandtl number ≤100. Results have shown that the wall temperature decrease with increasing the values of Prandtl number. The skin friction decreases with increasing Prandtl number. Increasing Prandtl number increase a detachment of the boundary layer. In addition to what we have juste said, Kumari and Pop [18] have investigated the free convection heat flux.

This study focuses on the modeling of heat and mass transfers around a rotating cone of revolution. Heat and mass transfers within boundary layers as well as pulse transfer have been considered. The Couette effect caused by the rotation of the cone that created heat and mass transfers is highlighted. Authors determine the distribution of velocity, temperature and concentration by solving systems of conservation algebraic equations using Thomas' algorithm. A detailed study of the mesh effect is undertaken resulted the selection of the most suitable mesh for this study. One analyzed the influence of the angular velocity of heat and mass transfer.

II. METHODOLOGY

A. *Physical Model*

Consider a fluid flowing in the vicinity of a cone of revolution rotating uniformly at angular velocity ω around its axis of revolution, completely immersed in a Newtonian fluid, in this case air initially at rest (*Fig.1*). The temperature and mass concentration of the fluid outside the thermal boundary layer are set to T_∞ and C_∞ respectively. Its wall is maintained at a uniform and constant temperature T_P and mass concentration C_0 and greater than the temperature T_∞ and concentration C_∞ of the fluid away from the surface. Let's associate with this cone a relative cartesian

coordinate system Oxyz whose origin O is placed at its summit. The abscissa x is counted positively away from the vertex and the ordinate y is perpendicular to the x axis. The axis of symmetry (Δ) is vertical and oriented in the opposite direction to the gravitational field. It is assumed that the system is initially in thermodynamic equilibrium. The rotation of the cone causes the temperature gradient between the fluid and the wall due to its dynamic viscosity. The heat gained by the fluid particles causes their temperature to rise. Fluid flow coupled with heat and mass transfer is created by the Couette effect. Thermal and mass external rotary convection then takes place in the fluid to re-establish thermodynamic equilibrium between the wall and the fluid.

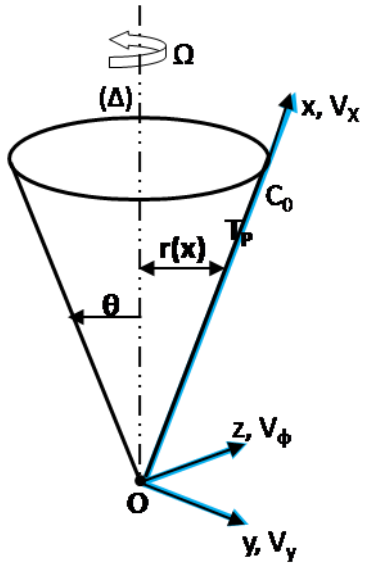

Fig.1. *Diagram of the physical model and coordinate system*

B. Mathematical Formulation

To model mathematically the phenomenon, the following assumptions are made:

- The flow is in a stationary laminar regime
- The flow is uniform away from the wall
- The fluid is Newtonian and incompressible
- The fluid is air, whose physical properties are constant .
- Radiation, viscous dissipation and the pressure term are neglected in the heat equation
- No other heat sources
- Heat and mass transfers occur exclusively in the boundary layers
- Species diffusion is mass based
- Force of gravity and force of pressure are zero
- The pressure inside the boundary layer is constant
- The cone wall is isothermal and impermeable

C. Dimensionless Equations

- Dimensionless variables

The dimensionless variables are defined as follows:

$$x^+ = \frac{x}{L}\,,\ y^+ = \frac{y}{L}\sqrt{Re_\omega}\,,\ r^+ = \frac{r}{L} \tag{1}$$

$$V_x^+ = \frac{V_x}{L\omega}Re_\omega^{\frac{1}{4}}\,,\ V_y^+ = \frac{V_y}{L\omega}Re_\omega^{\frac{3}{4}}\,,\ V_\varphi^+ = \frac{V_\varphi}{L\omega}Re_\omega^{\frac{1}{4}} \tag{2}$$

$$T^+ = \frac{T-T_\infty}{\left(\frac{L^2\omega^2}{2Cp}\right)}\,,\ C^+ = \frac{C-C_\infty}{C_0-C_\infty} \tag{3}$$

The dimensionless from of the governing equations are as following:

- Dimensionless continuity equation

$$\frac{\partial V_x^+}{\partial x^+} + \frac{\partial V_y^+}{\partial y^+} + \frac{V_x^+}{r^+}\frac{dr^+}{dx^+} = 0 \tag{4}$$

- Dimensionless momentum equations

$$V_X^+\frac{\partial V_X^+}{\partial x^+} + V_y^+\frac{\partial V_X^+}{\partial y^+} - \frac{{V_\varphi^+}^2}{r^+} = Re_\omega^{\frac{1}{4}}\frac{\partial^2 V_X^+}{\partial {y^+}^2} \tag{5}$$

$$V_X^+\frac{\partial V_\varphi^+}{\partial x^+} + V_y^+\frac{\partial V_\varphi^+}{\partial y^+} + \frac{V_X^+ V_\varphi^+}{r^+} = Re_\omega^{\frac{1}{4}}\frac{\partial^2 V_\varphi^+}{\partial {y^+}^2} \tag{6}$$

- Dimensionless heat transfer equation

$$V_X^+\frac{\partial T^+}{\partial x^+} + V_y^+\frac{\partial T^+}{\partial y^+} = \frac{1}{Pr}Re_\omega^{\frac{1}{4}}\frac{\partial^2 T^+}{\partial {y^+}^2} \tag{7}$$

- Dimensionless mass transfer equation

$$V_X^+\frac{\partial C^+}{\partial x^+} + V_y^+\frac{\partial C^+}{\partial y^+} = \frac{1}{Sc}Re_\omega^{\frac{1}{4}}\frac{\partial^2 C^+}{\partial {y^+}^2} \tag{8}$$

The dimensionless parameters in these equations are defined respectively as Schmidt number, Reynolds number and Prandlt number:

$$Sc = \frac{\mu}{\rho D}\,,\ Re_\omega = \frac{L^2\,\omega}{\nu}\,,\ Pr = \frac{\mu Cp}{\lambda} \tag{9}$$

The dimensionless boundary conditions are specified as follow:

$$y^+ = 0, V_X^+ = 0\,,\ V_y^+ = 0\,,\ V_\varphi^+ = r^+\,Re_\omega^{\frac{1}{4}} \tag{10.a}$$

$$T^+ = 1, C^+ = 1 \tag{10.b}$$

$$y^+ \to \infty\,,\ T^+ = 0\,,\ C^+ = 0, V_X^+ = 0, V_\varphi^+ = 0 \tag{10.c}$$

The dimensionless variables are defined as:

Eckert number: $Ec = \frac{(L\omega)^2}{Cp\,\Delta T}$ (11)

Nusselt number: $2\frac{Nu}{Ec\sqrt{Re_\omega}} = -\left(\frac{\partial T^+}{\partial y^+}\right)_{y^+=0}$ (12)

Sherwood number: $\frac{Sh}{\sqrt{Re_\omega}} = -\left(\frac{\partial C^+}{\partial y^+}\right)_{y^+=0}$ (13)

Longitudinal and azimuthal parietal friction coefficients are defined by:

$$\frac{1}{2}Cf_u\,Re_\omega^{\frac{3}{4}} = \left(\frac{\partial V_X^+}{\partial y^+}\right)_{y^+=0}, \frac{1}{2}Cf_w\,Re_\omega^{\frac{3}{4}} = \left(\frac{\partial V_\varphi^+}{\partial y^+}\right)_{y^+=0} \quad (14)$$

Mass diffusion rate at the wall is deduced from Fick's law:

$$VD_f = -\frac{D_f}{L}\frac{(C_0 - C_\infty)}{C_0}\sqrt{Re_\omega}\left(\frac{\partial C^+}{\partial y^+}\right)_{y^+=0} \quad (15)$$

The concentration of water vapor at the wall:

$$C_0 = \frac{0{,}622P_v}{P_{atm} - 0{,}378P_v} \quad (16)$$

P_v and P_{atm}: partial pressure of water vapor and atmospheric pressure.

Hr relative humidity of the air

$$P_v = Hr\ Pvs(Tp) \quad (17)$$

Saturation vapor pressure at temperature Tp

$$P_{vs}(Tp) = 10^{17{,}442 - \frac{2790}{Tp} - 3{,}868\log_{10}(Tp)} \times 101325 \quad (18)$$

Df : diffusion coefficient ($m^2\ s^{-1}$)

$$D_f = 2{,}17.10^{-5}\frac{P_0}{P}\left(\frac{T}{273{,}15}\right)^{1{,}88} \quad (19)$$

P_0: fluid pressure at T=273,15K

III. Numerical Methods

A. Discretisation and Algorithm

The conservation equations associated with the boundary conditions have discretized using an implicit finite difference method by considering meshes of 250 x 450 knots with $\Delta y^+ = 0.1$. After arrangement, the discretized (5) to (8) can be respectively put into the following forms:

$$Au_j V_{X_{j-1}}^+ + Bu_j V_{X_j}^+ + Cu_j V_{X_{j+1}}^+ = Du_j \quad (20.a)$$

$$Aw_j V_{\varphi_{j-1}}^+ + Bw_j V_{\varphi_j}^+ + Cw_j V_{\varphi_{j+1}}^+ = Dw_j \quad (20.b)$$

$$At_j T_{j-1}^+ + Bt_j T_j^+ + Ct_j T_{j+1}^+ = Dt_j \quad (20.c)$$

$$Ac_j C_{j-1}^+ + Bc_j C_j^+ + Cc_j C_{j+1}^+ = Dc_j \quad (20.d)$$

The system of algebraic equations (20.a) through (20.d) associated with the discretized boundary conditions can be solved by the Thomas algorithm.

$$A_j X_{j-1}^{i+1} + B_j X_j^{i+1} + C_j X_{j+1}^{i+1} = D_j \quad (21)$$

with $2 \le j \le J_{max}$, X represents the quantities ($V_X^+, V_\varphi^+, T^+, C^+$) and J_{max} characterizes the thickness of the boundary layer.

The convergence of the iterative process within the boundary layer is assumed to be achieved when the following criterion is simultaneously verified on $V_X^+, V_\varphi^+, T^+, C^+$ is:

$$\left|\frac{\max(X^{n+1} - X^n)}{\max(X^n)}\right| \le 10^{-3} \quad (22)$$

with n is iteration number, X = ($V_X^+, V_\varphi^+, T^+, C^+$)

The normal component V_y^+ is calculated from the discretized continuity equation:

$$V_y^+\binom{i+1}{j+1} = V_y^+\binom{i+1}{j} - \Delta y^+\left[\frac{V_X^+\binom{i+1}{j} - V_X^+\binom{i}{j}}{\Delta x^+} + \frac{V_X^+\binom{i+1}{j}}{\Delta x^+}\left(1 - \frac{r^+(i)}{r^+(i+1)}\right)\right] \quad (23)$$

Partial derivatives of the expressions of Nusselt, Sherwood and friction coefficients are approached by three points discretization:

$$2\frac{Nu}{Ec\sqrt{Re_\omega}} = -\frac{3T^+\binom{i+1}{j+1} - 4T^+\binom{i+1}{j} + T^+\binom{i+1}{j-1}}{2\Delta y^+} \quad (24)$$

$$\frac{Sh}{\sqrt{Re_\omega}} = -\frac{3C^+\binom{i+1}{j+1} - 4C^+\binom{i+1}{j} + C^+\binom{i+1}{j-1}}{2\Delta y^+} \quad (25)$$

$$\frac{1}{2}Cf_u\,Re_\omega^{\frac{3}{4}} = \frac{3V_X^+\binom{i+1}{j+1} - 4V_X^+\binom{i+1}{j} + V_X^+\binom{i+1}{j-1}}{2\Delta y^+} \quad (26)$$

$$\frac{1}{2}Cf_w\,Re_\omega^{\frac{3}{4}} = \frac{3V_\varphi^+\binom{i+1}{j+1} - 4V_\varphi^+\binom{i+1}{j} + V_\varphi^+\binom{i+1}{j-1}}{2\Delta y^+} \quad (27)$$

B. Meshes Effect

Table I gives the values of the Nusselt number for several mesh values. It shows that the number of Nusselt increases with the number of points following the meridian. But we see that it is independent of the number of points according to the normal.

TABLE I. Values of the Nusselt Number for different Meshes Values

Mesh	x^+		
	0.4	0.5	0.6
	Nu		
100 x 150	0.7850361	0.841595	0.8820879
150 x 250	0.8820863	0.837242	0.977429
250 x 400	1.0035023	1.060603	1.1092288
250 x 450	1.0035023	1.060603	1.1092288
400 x 450	1.1268802	1.189732	1.2432423
450 x 500	1.1596996	1.224075	1.2788707

In order to ensure mesh independence on the obtained results, we have considered different meshes 100 x 150, 150 x 250, 250 x 400, 250 x 450, 400 x 450 and 450 x 500 for $\Delta y^+ = 0.1$, ω = 15 rad/s and θ_0 = 20. The influence of the mesh on the Nu is presented in Table I. The results of our simulation show that the 250 x 400 mesh size is sufficient. This study of the effect of the mesh size allowed us to choose the 250 x 450 mesh size as a fine mesh size for the present study.

C. Validation

Our calculation code was validated on a natural and rotary mixed convection problem around a vertical cone. We have compared our results with those obtained by Hering and Grosh [3], Himasekhar et al.[1] and Anilkumar and Roy [5]. The comparison is about the gradient of azimuthal component parietal for the Richardson numbers Ri = 0 and angular velocity ω = 50π. The analysis in Table II shows that our results are in perfect agreement with the results available in the literature, the relative difference not exceeding 1%.

TABLE II. THE GRADIENT OF THE AZIMUTHAL COMPONENT PARIETAL

	Hering [3]	Himasekhar [1]	Anilkumar [5]	Present model
$-\left(\frac{\partial V_{\varphi}^{+}}{\partial y^{+}}\right)_{y^{+}=0}$	0.6159	0.6158	0.6160	0. 61584
Absolute relative gap	0.00006	0.00004	0.00016	

IV. RESULTS AND DISCUSSION

Numerical results are obtained for values of: Pr = 0.71,Sc = 0.62, Ec= 0.0025, Δy^{+}= 0.1and θ_0 = 20.

Fig. 2 shows the profile of the dimensionless meridian velocity V_x^+ as a function of y^+ for several values of x^+. The creation of this non zero value of the meridional component is due to the impulse caused by the rotation of the cone, which propagates in this direction. We observe a longitudinal upward movement of the fluid, so the fluid particles climb the wall. The fluid inside the thermal boundary layer is accelerated more than outside. This maximum of V_x^+ corresponds to the change in behaviour from real fluid to free fluid. We can see that the maximum value of V_x^+ rises along the wall and is an increasing function of the meridian abscissa.

Due to the Couette effect, the fluid particles in the immediate vicinity of the wall are entrained by the movement, which gives rise to the azimuthal component V_{φ}^+. Its variation as a function of y^+ for several values of x^+ is shown in *Fig. 3*. It is maximum at the wall, decreasing along the normal and tending towards zero at infinity. We can see that the adimensional azimuthal velocity increases as we move in the meridian direction but decreases along the normal. Furthermore, as we move up the wall of the cone, the radius of the circles parallel to the surface of the base and perpendicular to the axis of revolution increase, so the azimuthal component also increases.

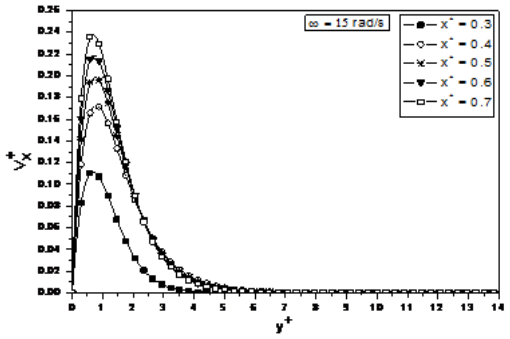

Fig. 2. *Reduced V_X^+ according to y^+ for several values of x^+.*

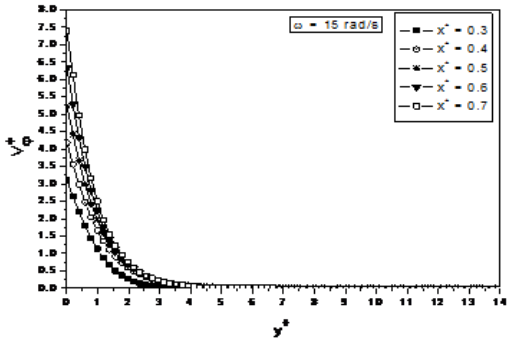

Fig.3. *Reduced V_{φ}^+ according to y^+ for several values of x^+.*

The Couette effect also creates the normal component, the variation of which is shown in *Fig. 4*. It shows that the velocity component V_y^+ decreases in the boundary layer with y^+. It takes on a negative value, which means that the fluid particles are sucked towards the axis of rotation of the cone, i.e., towards the wall. The suction effect is stronger than outside the dynamic boundary layer and increases along the wall.

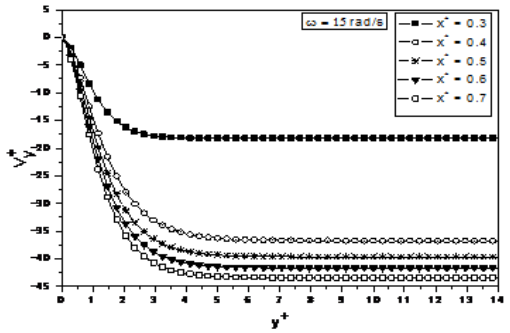

Fig. 4. *Reduced V_y^+ according to y^+ for several values of x^+*

Fig. 5 shows the variation in temperature as a function of y^+. The heat is localized near the wall of the cone. So, the fluid near the wall is hotter. The dimensionless temperature decreases because the Prandtl number is less than one. It decreases along the normal and the temperature gradient is very strong inside the thermal boundary layer. Fluid temperatures decrease along the cone wall because

the thickness of the thermal boundary layer is a decreasing function of the meridian abscissa.

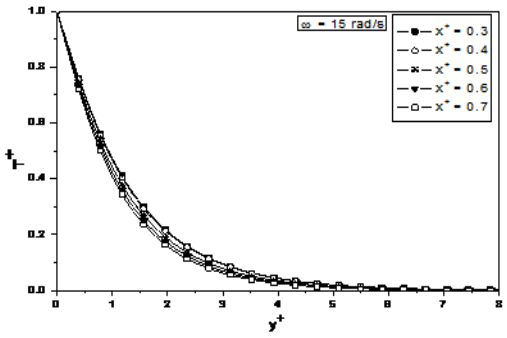

Fig.5. *Reduced temperature according to y^+ for several values* of x^+

Fig. 6 represents the variations of the dimensionless mass concentration as a function of y^+ for several values of x^+. The difference in concentration at the wall and to infinity creates a mass transfer. It shows that C^+ decreases with x^+ and the thickness of the mass boundary layer decreases along the wall. The mass is transferred from more concentrated regions to less concentrated regions.

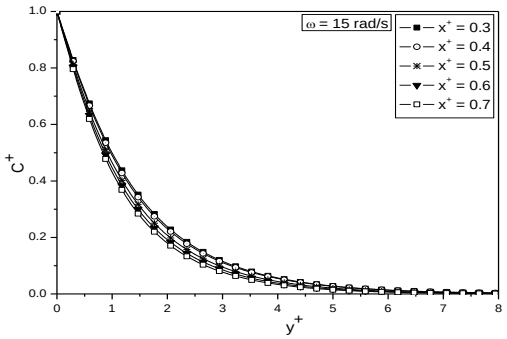

Fig. 6.*Reduced concentration mass according to $y^+$for several values of x^+*

Fig. 7 represents the variations of the Nusselt number as a function of x^+ for several values of ω. It shows that the intensity of the heat transfer between the wall and the fluid increases as one traverses the cone from the bottom to the top because of the gradually increasing difference in their temperatures. Moreover, $\frac{2\,Nu}{Ec\sqrt{Re_\omega}}$ it is a decreasing function of ω, that is to say that the higher the rotation, the less the heat transfer by convection has no time to be established and therefore less important.

Fig. 8 illustrates the evolution of the number of local Sherwood for different values of ω as a function of x^+, the number of Sherwood characterize the transfer of mass. The mass transfer between the wall and the fluid increases along the wall. The dimensionless quantity $\frac{Sh}{\sqrt{Re_\omega}}$ decreases with increasing of the velocity.

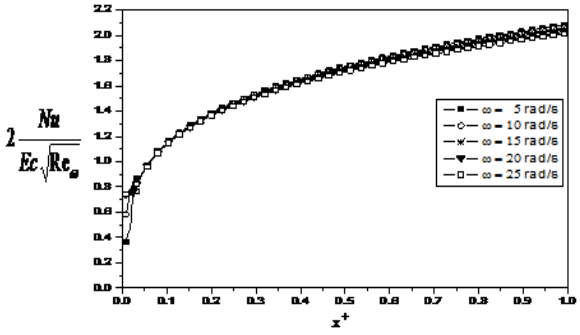

Fig.7. *Evolution of the Nusselt number as a function of x^+ for several values of ω*

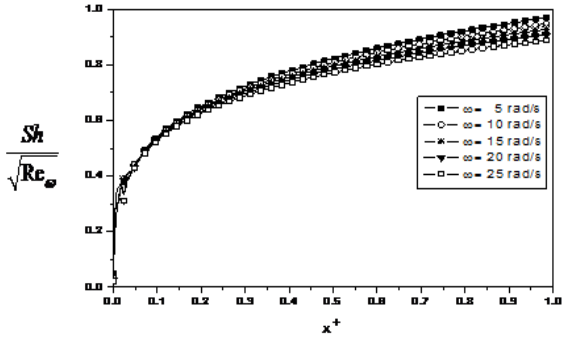

Fig.8. *Evolution of the Sherwood number as a function of x^+ for several values of ω*

Table III gives the values of the longitudinal and azimuthal dimensional friction coefficients for several values of x^+ with $\Delta y^+ = 0.1$, ω = 15 rad/s and $\theta_0 = 20$. It shows that the values of $\frac{1}{2}Cf_u Re_\omega^{\frac{3}{4}}$ are positive while those of $\frac{1}{2}Cf_w Re_\omega^{\frac{3}{4}}$ are negative. This means that the fluid adheres longitudinally and there is azimuthal detachment of the dynamic boundary layer.

TABLE III. THE VALUES OF LONGITUDINAL AND AZIMUTHAL PARIETAL FRICTION COEFFICIENTS

x^+	$\frac{1}{2}Cf_u Re_\omega^{\frac{3}{4}}$	$\frac{1}{2}Cf_w Re_\omega^{\frac{3}{4}}$
0.01	0.01815	- 0.03709
0.1	0.10858	- 0.67055
0.2	0.17474	- 1.5957
0.3	0.22533	- 2.6366
0.4	0.26729	- 3.7581
0.5	0.30348	- 4.942
0.6	0.33543	- 6.1773
0.7	0.36409	- 7.456
0.8	0.39007	- 8.7727
0.9	0.41383	- 10.123
1	0.43359	- 11.364

The variation of the mass diffusion rate as a function of x^+ for several values of ω is shown in *Fig. 9*. Increasing the rotational speed increases the mass diffusion rate because the gradient of the fluid concentration is an increasing function of the angular velocity.

Fig. 10 shows the variation of the mass diffusion rate as a function of x^+ for several values of Hr. Air vapor saturation increases with relative humidity. The mass diffusion rate increases with increasing of the relative humidity because the saturation vapor pressure increases with increasing relative humidity

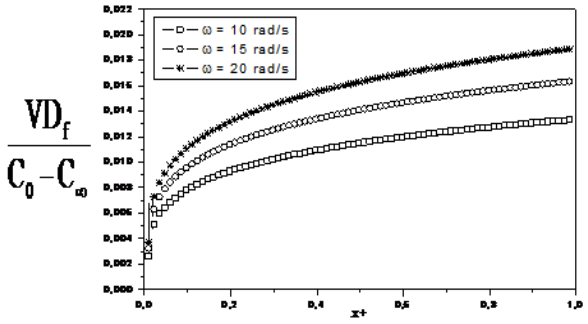

Fig. 9. *Variation of the mass diffusion rate as a function of x^+ for several values of ω (Hr =65%)*

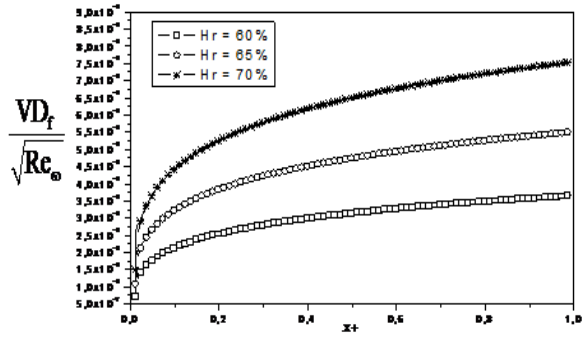

Fig. 10. *Variation of the mass diffusion rate as a function of x^+ for several values of Hr (ω=15rad/s)*

In rotary convection, the Nusselt and Sherwood numbers are function of the rotational Reynolds number and the meridian abscissa. The Nusselt and Sherwood correlations can be written in the form as follow:

$$Nu(x)=a\,Pr^{b}\,Re_{\omega}^{c}\,(x^{+})^{d} \text{ and } Sh(x)=a\,Sc^{b}\,Re_{\omega}^{c}\,(x^{+})^{d}$$

The constants a, b, c, and d are determined by smoothing, using the least squares method of the curve of Nusselt and Sherwood numbers have a function of x^+, see *Figs.11* and *12* below. In our case, we get the local correlations of Nusselt and Sherwood number according to x^+ and of Re_{ω} as follow:

$$Nu(x)=0.0016\sqrt{Re_{\omega}}\left(\frac{1}{Pr}\right)\left(x^{+}\right)^{0.2} \quad (28)$$

$$Sh(x)=0.52\sqrt{Re_{\omega}}\left(\frac{1}{Sc}\right)\left(x^{+}\right)^{0.2} \quad (29)$$

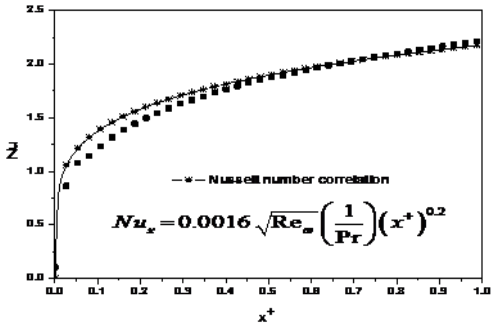

Fig. 11. *Evolution of the Nusselt number correlation as a function of x^+ (θ_0 = 20, ω=15 rad/s)*

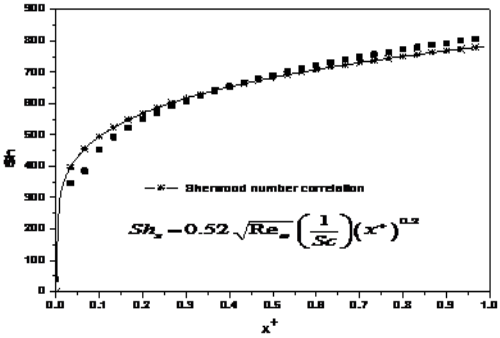

Fig. 12. *Evolution of the Sherwood number correlation as a function of x^+(θ_0 = 20, ω=15 rad/s)*

V. CONCLUSION

Heat and mass transfer around a rotating cone have been modeling. Mathematical model based on the heat, mass transfer, Navier-Stokes and continuity equations coupled implicit finite difference scheme technique has been established. THOMAS algorithm has been used to solve the algebraic equations system associated with boundary conditions to determine the distributions of temperature, velocity, and mass concentration.

One concludes that the rotation of the cone around its axis of revolution, by Couette effect, creates a meridian velocity component that causes an upward flow inside the dynamic boundary layer. The normal component takes the negative value so the fluid is exposed to suction. In fact, the fluid is returned to the wall. As a result, it produces the suction of the fluid. It also creates a flow of fluid in which a concentration boundary layer develops. Analysis of T^+ and C^+ variations shows that the thickness of the thermal boundary layer is smaller than that of the mass boundary layer. The thermal and mass transfer rates increase along the wall. At the stopping point, there are small Nusselt and Sherwood numbers. In the upper meridians, near the point of separation, the

Nusselt and Sherwood numbers are considerable. The transfer rates evolve in the same direction, as do the temperature and the mass concentration. The heat transfer rate is greater than the mass transfer rate. Heat transfer is more dominant than mass transfer. The angular velocity of the cone positively influences heat and mass transfer. An increase in relative humidity increases the mass diffusion rate. It shows us that the importance of mass diffusion is at the same direction as that of the relative humidity of the air. The correlations of Nusselt and Sherwood numbers for a given opening of the cone have been proposed.

ACKNOWLEDGMENT

Author would like to thank the team of the Laboratory of Mechanics Energetic and Environment for their collaborations.

REFERENCES

[1] K. Himasekhar, P.K. Sarma, and K. Janardhan, "Laminar mixed convection from a vertical rotating cone," International Communication Heat Mass Transfer, vol.16, no.1, pp. 99 – 106, 1989.

[2] T.Y. Wang, C. Kleinstreuer, and H. Chiang, "Mixed convection from a rotating cone with variable surface temperature," Numerical Heat Transfer, Part A: Applications, vol.25, no.1, pp. 75-83, 1994.

[3] R.G. Hering and R.J. Grosh, "Laminar combined convection from a rotating cone," Journal of Heat Transfer, Trans. ASME, Series C, vol. 85, pp. 29, 1963.

[4] M.Y. Malik, H. Jamil, T. Salahuddin, S. Bilal, K.U. Rehman, and Z. Mustafa, "Mixed convection dissipative viscous fluid flow over a rotating cone by way of variable viscosity and thermal conductivity," Results in Physics, vol.**6**, pp.1126 -1135, 2016.

[5] D. Anilkumar and S. Roy, "Unsteady mixed convection flow on a rotating cone in a rotating fluid," Applied Mathematics and Computation, vol.155, pp. 545-561, 2004.

[6] S. Saleem, "Heat and mass transfer of rotational flow of unsteady third grade fluid over a rotating cone with buoyancy effects, "Hindawi Mathematical Problems in Engineering, pp.1-9, 2021.

[7] B.R. Sharma and H. Konwar, "Flow, heat and mass transfer about a permeable vertical rotating cone, " International Journal of Fluids Engineering, vol. 7,no.1, pp. 25 – 40, 2015.

[8] P.M. Patil and I. Pop, "Effects of surface mass transfer on unsteady mixed convection flow over a vertical cone with chemical reaction," Heat Mass Transfer, vol.47, pp. 1453 – 1464, 2011.

[9] Y.C. Ching, "Free convection heat transfer from a non isothermal permeable cone suction and temperature dependent viscosity," Journal of Applied Science and Engineering, vol. 18, no.1, pp. 17–24, 2015.

[10] A.H. Srinivasa and A.T. Eswara, "Unsteady free convection flow and heat transfer from an isothermal truncated cone with variable viscosity," International Journal of Heat and Mass Transfer, vol. 57, pp. 411– 420, 2013.

[11] P. Bapuji, K. Ekambavanan, and A.J. Chamkha, "Unsteady laminar free convection from a vertical cone with uniform surface heat flux," Nonlinear Analysis: Modelling and Control, vol.13, no.1, pp. 47-60, 2008.

[12] M. Kumari, I. Pop, and G. Nath, "Mixed convection along a vertical cone," International Communication Heat Mass Transfer, vol.16, no. 2, pp. 247 – 255, 1989.

[13] P. Bapuji and A.J. Chamkha, "Numerical solutions of unsteady laminar free convection from a vertical cone with non-uniform surface heat flux," Journal of Applied Fluid Mechanics ,vol.6, no.3, pp. 357 – 367, 2013.

[14] R. Azad, M.M. Molla, and M.M.A. Sarker, "Natural convection flow along the vertical wavy cone in case of uniform surface heat flux where viscosity is an exponential function of temperature," International Communications in Heat and Mass Transfer, vol 38, pp. 774 – 780, 2011.

[15] T. Sharaban, A. Rahman, M.M. Molla, and M. M.A. Sarker, "Effects of temperature dependent thermal conductivity on natural convection flow along a vertical wavy cone with heat flux," Procedia Engineering, vol 90, pp. 497–503, 2014.

[16] P. Bapuji, K. Ekambavanan, and A.J. Chamkha, "Unsteady laminar natural convection flow past an isothermal vertical cone, "Heat and Technology, vol 25, no. 2, pp.17-28, 2007.

[17] F.N. Lin, "Laminar free convection from a vertical cone with uniform surface heat flux," Lettres in Heat and Mass Transfer , vol. 3, no. 1, pp. 49 - 58. , 1976.

[18] M. Kumari and I. Pop, "Free convection over a vertical rotating cone flow, heat and mass transfer about a permeable vertical rotating cone with constant wall heat flux, " Applied Mechanics and Engineering , vol.3, no.3, pp. 451-464,1998.